
This is the **accepted version** of the article:

Kováč, Daniel; Veselá, Barbora; Klem, Karel; [et al.]. «Correction of PRI for carotenoid pigment pools improves photosynthesis estimation across different irradiance and temperature conditions». *Remote sensing of environment*, Vol. 244 (July 2020), art. 111834. DOI 10.1016/j.rse.2020.111834

This version is available at <https://ddd.uab.cat/record/224227>

under the terms of the  license

1 Correction of PRI for carotenoid pigment pools improves photosynthesis estimation across different
2 irradiance and temperature conditions

3 Daniel Kováč¹, Barbora Veselá¹, Karel Klem¹, Kristýna Večeřová¹, Zuzana Materová Kmecová², Josep
4 Peñuelas^{1,3,4}, Otmar Urban¹

5 ¹Global Change Research Institute of the Czech Academy of Sciences, Bělidla 986/4a, 603 00 Brno,
6 Czech Republic

7 ²Faculty of Science, Ostrava University, 30. dubna 22, 701 03 Ostrava 1, Czech Republic

8 ³CSIC, Global Ecology Unit CREAM-CSIC-UAB, E-08193 Bellaterra (Catalonia), Spain

9 ⁴CREAF, E-08193 Cerdanyola del Vallès (Catalonia), Spain

10 **Abstract**

11 We studied the influence of changing carotenoid pigments on the sensitivity of the photochemical
12 reflectance index (PRI) to photosynthesis dynamics. The goal of the measurements was to examine
13 how the introduction of Δ PRI into the working dataset can improve the estimation of photosynthesis.
14 Spectral and photosynthetic characteristics of European beech and Norway spruce saplings were
15 periodically measured in growth chambers with an adjustable irradiance and temperature. Patterns of
16 environmental changes inside the growth chambers were created by periodic changes in irradiance
17 and temperature. Four general irradiance periods lasting 10-12 days each were established. Introduced
18 irradiance regimes varied in the sum of daily irradiance and amplitude of irradiance changes.
19 Temperature was changed with more complex patterns to induce changes in xanthophyll cycle
20 pigments at various time scales within these regimes. Our measurements confirmed the PRI linkage to
21 photosynthetic light use efficiency (LUE). However, the strength of this connection was found to be
22 dependent on changing pigment concentrations, specifically on the change in the ratio of chlorophylls
23 to carotenoids. Furthermore, a negative interference in photosynthesis estimation from PRI was

24 recorded if the temperature was lowered overnight to 12° C. The differential PRI (Δ PRI), calculated as
25 the simple difference between the PRI value measured during the daytime period and in early morning
26 (PRI_0), revealed a decreased effect from pigments and cold temperature on LUE estimation. The
27 regression analysis among all measured data identified an increased association between PRI and LUE
28 following the introduction of Δ PRI from $R^2 = 0.26$ to 0.69 in beech and from $R^2 = 0.61$ to 0.77 in spruce
29 data. The analyses showed that both leaf carotenoid concentrations and the conversion state of
30 xanthophyll cycle pigments played a significant role in determining PRI and PRI_0 values and that the
31 accurate assessment of these pigments in PRI across multiple levels of stress from irradiance and
32 temperature might improve estimations of LUE through Δ PRI. In our data, Δ PRI appeared to be a good
33 measure of photosynthesis, the dynamics of which differed between beech and spruce saplings upon
34 switching temperatures.

35 KEYWORDS: photochemical reflectance index, proximal sensing, irradiance, temperature, carotenoids,
36 xanthophyll cycle, light use efficiency

37 1 | INTRODUCTION

38 The usefulness of a photochemical reflectance index (PRI) approach to link plant photosynthetic CO₂
39 uptake efficiency in changing light (light use efficiency, LUE) and remotely sensed data has been widely
40 reported (Garbulsky et al., 2008; Peñuelas et al., 2011). PRI is based on our understanding of the
41 photoprotective role of xanthophyll cycle pigments within plants. When plants absorb more light
42 energy than can be used by chlorophyll to produce glucose, excessive light energy is either transferred
43 to xanthophyll molecules and emitted as heat or emitted as fluorescence (Gamon et al., 1992; Rascher
44 et al., 2009). Variations in xanthophyll cycle pigment concentrations and conversions produce
45 reflectance changes at a wavelength of 531 nm. Comparing this reflectance with a reference
46 wavelength (typically 570 nm) can be used to detect stress (Gamon et al., 1997, 1992; Peñuelas et al.,
47 1995). Examination of empirical work has determined a fundamental relationship between plant
48 photochemistry and PRI that is based on the responsiveness of photosynthesis to irradiance.

49 The variability of factors that may affect canopy-measured PRI can produce confusion in interpreting
50 PRI, in addition to the desirable effects introduced by changing pigments. In field applications, sun–
51 canopy–sensor geometry can exert a strong effect on the resulting PRI values, as light fields may vary
52 in complex ways with canopy structure (Middleton et al., 2009; Sims et al., 2006). Wu et al. (2015)
53 examined crops and found the structural dependence of PRI on leaf area index (LAI). In addition, these
54 authors proposed a solution for removal of the structural signal, and their results imply that LAI change
55 as a consequence of a change in the illumination angle can impact the measured PRI of the canopy.
56 The results reported by Wu et al. (2015) and Gitelson et al. (2017) suggest that canopy structure-
57 related LAI interferences should be considered when evaluating PRI responses between canopies with
58 lower LAI.

59 The foliar ratio of chlorophylls to carotenoids ($Chla+b/Carx+c$) has a strong impact on the observed PRI
60 variability (Filella et al., 2009). Decreasing $Chla+b/Carx+c$ may be related to photosynthesis
61 downregulation in stressed plants, but the changes in pigments may also cause impairment of the PRI–
62 LUE relationship over the long term. Attempts have been made to eliminate the $Chla+b/Carx+c$
63 variability in the measured signal by deconvoluting the influence of pigments. Gamon and Surfus
64 (1999) have shown an opportunity to detract the extent of xanthophyll cycle pigment conversions by
65 subtracting measured PRI value from the starting PRI value in introduced ΔPRI ($\Delta PRI = PRI_0 - PRI$).
66 Following this work, Gamon and Berry (2012) characterized differences in ΔPRI between sun and shade
67 leaves as induced with pigment changes. This study has shown that PRI_0 represents a PRI state to which
68 PRI values can be related if the comparison of diurnal changes and plant groups is required. Ideally,
69 PRI_0 is measured at low irradiance on leaves with inactivated protective functions to isolate the slow
70 changing component of PRI most likely related to $Chla+b/Carx+c$ and the concentration of lutein
71 pigments. Magney et al. (2016) determined that the ΔPRI does respond to diurnal physiological
72 changes resulting from changes in VPD, air temperature, and stomatal conductance and suggested
73 that these changes may be dependent on the observed pigment dynamics. Nitrogen availability
74 affecting amounts of chlorophylls was considered a primary driver of ΔPRI sensitivity in this study,

75 defining the slope of the observed dependency. Δ PRI yields better correlations in nutrient-deficient
76 plots, thereby indicating the importance of carotenoid levels in observed relationships. There are
77 several good examples showing the opportunity to better estimate LUE from PRI measured at the top
78 of the canopy, if the value of PRI is corrected to the morning PRI_0 (Hmimina et al., 2015, 2014; Ripullone
79 et al., 2011; Soudani et al., 2014). The presented studies often involve drought stress in the
80 experimental design as the main factor driving photosynthesis declines and the magnitude of PRI
81 response (Magney et al., 2016). We intend to further study the basics of the improved relationship
82 between photosynthetic LUE and Δ PRI, and the desirable role of changing pigments in developing
83 these relationships under conditions involving induced changes in irradiance and temperature.

84 Differences in the sensitivity of photosynthetic processes to light and temperature stress among
85 species suggest the occurrence of interactive effects on photosynthetic pigments. An insufficient
86 understanding of the associated reflectance signature in relation to the measure of photosynthesis is
87 consequential (Ollinger, 2011; Sims and Gamon, 2002). The co-variation of environmental drivers in
88 the upper canopy suggests that leaves in the upper canopy are often exposed to greater stress
89 originating from exposure of leaves to direct light (Niinemets and Valladares, 2004). Upper canopy
90 leaves may suffer from a variety of additional stresses, among which temperature stress may play a
91 particularly substantial role (Williams et al., 1996). The upper canopy crown, usually accounted for in
92 spectrometric measurements, may represent a substantial portion of the canopy involved in the
93 observed gas exchange (Coops et al., 2017). However, the functional trait attributes of plants may not
94 be the only features able to explain changes in PRI in a given environment. It may also be necessary to
95 account for the PRI variations with changing $Chla+b/Carx+c$ that determines the constitutive (slow-
96 changing) component of the PRI. It has been suggested that the finer definition of the facultative
97 process (fast-changing with xanthophyll cycle) can help to detect LUE and responses to summer stress,
98 such as heat and drought (Gamon and Bond, 2013). Our previous development provided elementary
99 knowledge of PRI changes in relation to dynamic fluctuations of photosynthetically active radiation
100 (PAR) and temperature (Kováč et al., 2018). This study suggests large improvement in estimating LUE

101 from Δ PRI, with measurements of PRI₀ that correspond to the xanthophyll cycle pigment conversion
102 state in the dark. Changes in PRI–LUE and Δ PRI–LUE relationships have yet to be investigated with
103 dynamic irradiance increases and temperature changes occurring on a daily scale.

104 We aimed to study further the sensitivity of both PRI and Δ PRI to decreasing and increasing
105 photosynthesis in fluctuating environments. In this study, we focused on observations of the effect of
106 mutual interactions among the plant pigments and overall canopy LAI on the developing relationship
107 between PRI and LUE in changing temperature conditions. Understanding the aspects of LUE
108 estimations using PRI would improve the applicability of PRI measurements in remote-sensing
109 applications. We aimed to overcome the canopy structural effect on measured PRI by fixing the
110 illumination–observation setup of the measurement by measuring canopies within the closed
111 environment of a growth chamber. We thus compared responses in photosynthesis, pigments and PRI
112 of tree species with distinctive sensitivities to low and high temperatures. Norway spruce trees, which
113 prefer cold regions and higher altitudes, were compared with European beech trees, which show
114 tolerance to higher temperatures and grow at lower altitudes. We established four regimes that varied
115 in their daily sum of irradiance income even as the trees were undergoing similar periodic changes in
116 temperature on a daily scale. We measured how the changes in pigments within these regimes
117 affected the observed PRI–LUE relationship and examined the role of established pigment
118 concentrations in the developing sensitivity of PRI and Δ PRI to LUE.

119 **2 | MATERIALS AND METHODS**

120 **2.1 | Setup of the experiment**

121 For the study, we selected two tree species with different habitat preferences: European beech (*Fagus*
122 *sylvatica*) and Norway spruce (*Picea abies*). These species are widespread within the Czech Republic
123 and the Central European region, with a distribution generally occurring according to their contrasting
124 climate and temperature demands. Seedlings of the selected tree species aged 3–4 years old (0.5–0.6
125 m tall) were grown in pots in the garden of the Global Change Research Institute from early spring until

126 the new leaves or needles were well developed. Thereafter, the trees were moved to the experimental
127 setting of growth chambers FS-SI-4600 (Photon Systems Instruments, Drásov, Czech Republic), where
128 they were processed for reflectance data acquisition, foliar photosynthetic pigments estimation and
129 photosynthesis measurements under changing conditions of irradiance (PAR) and temperature. The
130 initial acclimation period lasting 1 week (photoperiod 14 hours, irradiance $100 \mu\text{mol m}^{-2} \text{s}^{-1}$, day/night
131 temperatures set to 23/18°C and relative air humidity of 65%/80%) was followed with individual
132 regimes that differed in the sum of daily irradiance income, daily amplitude of irradiance changes and
133 temperature dynamics. Four periods of 10–12 days were established that varied in daily irradiance
134 amplitudes of 300–600–1200 (IRR1), 600–900–1500 (IRR2), 900–1200–1500 (IRR3), and 300–600–900
135 (IRR4) $\mu\text{mol m}^{-2} \text{s}^{-1}$. Detailed descriptions of irradiance and temperature changes according to time of
136 day within each regime are provided in the attached research data. The second day of each irradiance
137 period IRR1–IRR4 was established as a control day to measure plant responses to what can be termed
138 “standard” temperature changes following the irradiance fluctuations. The last 2 days of each
139 irradiance period were devoted to measuring parameters in fluctuating temperatures. The first day of
140 this 2-day measurement period started with the same temperature as on the previous day. The
141 temperature was then experimentally lowered at midday to 16 °C. This decreasing temperature was
142 started after the trees had been heated for half an hour during the midday period of highest PAR. The
143 temperature decrease to 16 °C was gradual over a period of 2 h (12:00 to 14:00). Temperature was
144 lowered compared to previous days as well as during the dark (night) period to 12°C. Cold period
145 temperatures remained the same for each irradiance regime. Heating after a cold period was started
146 during the morning of the following day. During that following day, the temperature was increased
147 compared to the previous control days while the irradiance level remained unchanged. Ranges of the
148 temperature change on normal days of IRR1–IRR4 were 20–26° C, 24–30° C, 25–35° C, and 19–24° C.

149 In the morning of each measuring day before the lights in the growth chambers were switched on, the
150 leaves and needles of beech and spruce saplings were collected for the estimation of foliar
151 photosynthetic pigments (Chl*a+b*, Car*x+c*) and individual carotenoid concentrations (antheraxanthin

152 (A), violaxanthin (V), zeaxanthin (Z)). Concentrations of chlorophylls and carotenoids were estimated
153 spectrophotometrically using a Specord 500 spectrophotometer (Analytik Jena, Jena, Germany).
154 Pigment concentrations in pigment extracts have been estimated from absorbance curves using
155 Lichtenthaler equations (1987). Amounts of xanthophyll cycle pigments were estimated by the HPLC
156 method (Kurasová et al., 2003), and the conversion state of the xanthophyll cycle pigments (i.e., de-
157 epoxidation state, or DEPS) was calculated according to Gilmore and Björkman (1994) as $DEPS = (A +$
158 $Z) / (V + A + Z)$. The maximum quantum yield of photosystem II photochemistry (F_v/F_m) was estimated
159 from measurements using a PAM-2500 portable chlorophyll fluorometer (Heinz Walz, Effeltrich,
160 Germany) for dark adapted leaves. The F_v/F_m was calculated as $F_v/F_m = (F_m - F_0)/F_m$, in which F_0 and
161 F_m represent the minimum (F_0) and maximum (F_m) chlorophyll fluorescence of darkness-adapted
162 leaves.

163 Reflectance factors of canopies created by four saplings of either beech (in July-August) or spruce
164 (September-October) species were measured in the growth chambers using a custom-made system
165 for measuring reflectance that is based on two JAZ spectrometers (Ocean Optics, Dunedin, FL, USA).
166 The spectrometric system is used for measurements in the dual field of view configuration. The trees
167 that were measured with a spectrometer were not moved throughout the measurement period. Each
168 JAZ unit measures data in spectral range between 340 and 1025 nm in 2048 channels with a spectral
169 resolution (FWHM) of 1 nm for each channel. The reflectance estimation was based on comparisons
170 between the radiant flux reflected from the measured canopy and incident (reference) irradiance at
171 each measuring wavelength similar to Gamon et al. (2015). Optimization of the measurement system
172 for measurements in growth chambers was performed using a spectralon panel reflecting a down-
173 welling radiant flux at PAR of $1500 \mu\text{mol m}^{-2} \text{s}^{-1}$. In addition, the radiance data estimation accounts for
174 the optimization of the signal measured using each unit to integration time to strengthen the signal-
175 to-noise ratio, conversion of the measured digital photon count signal to radiometric units, and dark
176 current spectrum correction of this signal. All the supporting information for the calculations of
177 reflectance factors from the measured data using the current establishment of the spectrometer,

178 optical fibres (2-meter-long QP600-UV-VIS optical fibres), and cosine reduction (CC-3-UV-T) was
179 estimated prior to initiating the measurements. The correction data were loaded into the measuring
180 system (on a desktop computer attached to the spectrometer), which processed the measured data
181 automatically while saving as text files the basic outputs from each data measurement. The
182 spectrometric method used for measuring reflectance factors is described in greater detail by Kováč
183 et al. (2018). The system setup ensured automatic data acquisition, starting in the morning and
184 continuing at a 1-minute frequency throughout the day. The computer connected to the
185 spectrometers via the USB port controlled simultaneous measurements by both spectrometers. The
186 LED Fyto-Panels (Photon Systems Instruments) that create the light environment inside the growth
187 chambers (Fig. 1) also served as the light source for measuring canopy reflectance factors. The linear
188 change in the light intensity produced by the Fyto-Panels enabled the measurement of canopy
189 reflectance factors without impacting the illumination directions and shadow fractions of vegetation
190 while changing the irradiance. As a result, we could attribute the variability in reflectance to pigment
191 changes in the measured leaves rather than to changes in canopy shadows as a consequence of
192 changing illumination angles. The sampled area covering four tree crowns was ca. 44 cm in diameter,
193 which was provided by the optical-fibre tip's 23° field of view and the 1-metre distance between the
194 trees and measuring optics. Examples of measured reflectance curves are shown in Fig. 1. PRI was
195 calculated following Gamon et al. (1997) as $PRI = (R_{531} - R_{570}) / (R_{531} + R_{570})$ from reflectance at
196 wavelengths of 530.37, 530.73, 531.08, 531.44, 531.79 nm (average used to estimate the value of R_{531}),
197 and 570.31, 570.67, and 571 nm (R_{570}). Development of PRI during the day period on control days
198 within each IRR regime is shown in Fig. 2. The average of the PRI data in the final 5 minutes of the initial
199 low-PAR period (under $100 \mu\text{mol m}^{-2} \text{s}^{-1}$) was taken as a PRI_0 value because a small rise in PRI was
200 always observed in response to activating the photosynthesis functions in the morning. Based on the
201 PRI_0 value, a differential PRI was later calculated as $\Delta PRI = PRI - PRI_0$ (Gamon and Berry, 2012) for each
202 PRI acquisition during the day.

203 The main focus of the gas-exchange measurement was to estimate the actual photosynthesis rate (A),
204 stomatal conductance (G_s), and transpiration (T_r). Measurements were collected five times per day at
205 PAR set at 300, 600, 900, 1200, or 1500 $\mu\text{mol m}^{-2} \text{s}^{-1}$ and at temperatures that were adjusted
206 accordingly. A portable photosynthesis system LI-6400 XT (LI-COR Biosciences, Lincoln, NE, USA) was
207 used to measure the photosynthetic dynamics of leaves in the upper crown. Leaves were measured
208 inside an LI-6400-02B leaf assimilation chamber. The light use efficiency (LUE) was calculated as $\text{LUE} =$
209 A/PAR . Within each IRR regime, gas exchange and chlorophyll fluorescence were initially measured on
210 the second day, referred to as the control day, and later on two consecutive days with induced cooling
211 of trees towards the end of each irradiance regime. The actual quantum yield of photosystem II
212 photochemistry (Φ_{PSII}) was calculated from PAM-2500 estimated values of steady state fluorescence
213 (F_s) and light-adapted maximum fluorescence (F_m') as $\Phi_{\text{PSII}} = (F_m' - F_s)/F_m'$ (Genty et al., 1989) for
214 each gas exchange data acquisition. Similarly, non-photochemical fluorescence quenching (NPQ) was
215 calculated as $\text{NPQ} = (F_m - F_m')/F_m'$. Photochemical fluorescence quenching (qP) was calculated as qP
216 $= (F_m' - F_s)/(F_m' - F_0')$ from F_s , F_m' and light-adapted minimum fluorescence (F_0'). A database was
217 created of spectrometric and physiology data measured under irradiances ranging from 300–1500
218 $\mu\text{mol m}^{-2} \text{s}^{-1}$ and temperature ranging from 14–35° C. The core data are available online.

219 **2.2 | Data analysis**

220 All analyses of the collected data were performed using R 3.5.1 (R Foundation for Statistical Computing,
221 Vienna, Austria). To visualize and quantitatively summarize the multivariate covariation of optical
222 variables (PRI and ΔPRI), major vectors of environmental factors, leaf pigment concentrations, and
223 physiology measures, we performed a principal component analysis (PCA). Principal component 1 and
224 2 scores were plotted in a PCA biplot. PCA analysis and visualization were conducted using the R
225 “factoextra” and “ggplot2” packages. The data for the individual parameters were tested for normality
226 using the Kolmogorov–Smirnov test. Tukey’s HSD post hoc ($p < 0.05$) multiple range test was performed
227 using the HSD.test function in the “agricolae” package to evaluate differences between individual

228 treatments. Data for the Tukey analyses are displayed in bar plot figures. A logarithmic regression
229 model was used to study the relationships among PRI, Δ PRI, and LUE at probability levels $p < 0.05$, $p <$
230 0.01 , and $p < 0.001$. Scores of regression analyses among the data within the individual IRR regimes
231 and between all data are shown in Table 1, and fitted logarithmic equations for pairs of data are shown
232 in Table 2. Dependency graphs between these key variables are displayed in Fig. 8.

233 **3 | RESULTS**

234 **3.1 | Relationships among environmental, optical, and physiological variables**

235 Principal component 1 (PC1) explained 37.6% of the total variation in European beech and 38.9% of
236 the total variation in Norway spruce data (Fig. 3). The functional traits responded significantly to PAR.
237 PAR determines the positions of individual values on the variable factor map, with individual data
238 points measured at low irradiances situated towards the bottom, negative part of the axis, whereas
239 data measured under high irradiances ($1500 \mu\text{mol m}^{-2} \text{s}^{-1}$) are situated towards the opposite end of
240 the graph. Even though trait responses to PAR showed general trends that were common to both
241 species, responses for both species were positioned on a gradient ranging from those that did not
242 respond significantly (with a closer link to PC2) to those that displayed high PAR trait plasticity. The
243 analysis showed that PAR differences were a common factor in determining the distribution of Φ_{PSII} ,
244 qP, LUE, and Δ PRI on the variable factor map. High PAR values produce low photochemical quenching
245 and LUE values and extremely negative Δ PRI values. The impact of PAR on values of PRI and NPQ was
246 still significant, but the relationship among PAR, PRI, and NPQ was weaker than expected (calculated
247 from research data). PRI was the only variable with a link to PC1, which showed a strong correlation to
248 $\text{Chl}a+b/\text{Car}x+c$ belonging to PC2 with a coefficient of correlation (R) equal to 0.89 ($p < 0.001$) in the
249 beech data set and 0.58 ($p < 0.001$) in the spruce data (calculated from research data). The lower LAI
250 of the beech canopy produced deeper amplitudes of PRI (Fig. 2) and resulted in a higher correlation
251 between $\text{Chl}a+b/\text{Car}x+c$ and PRI.

252 Principal component 2 (PC2) explained 23.8% of the total PCA variation in European beech and 25.2%
253 of that in Norway spruce data (Fig. 3). The main factors *A*, *Tr*, and *Gs* were placed in the lower and
254 upper quadrants of the PCA biplots in beech and spruce, respectively staying in contrast to the position
255 of temperature vector. This difference in directionality of *A*, *Tr* and *Gs* vectors is likely associated with
256 species specific sensitivity of photosynthesis to temperature variations. The opposite temperature
257 effects on the regulation of photosynthesis were reflected also in the directionality of the adjacent
258 *Chla+b/Carx+c* and PRI vectors.

259 **3.2 | Factors affecting the development of PRI and ΔPRI**

260 The two principal components in the PCA plots comparing early morning (before 8:00) values of
261 selected parameters to midday values (Fig. 4) explained approximately 64% of variability in the tested
262 data. The dependencies in the graphs could be rotated according to significance of predictors, but the
263 basic relationships among the measured data were similar between the species. Key relationships
264 among midday values of PAR, Φ_{PSII} , LUE and ΔPRI were similar to those identified among all the data in
265 Fig. 3. NPQ showed a link to midday PRI, which was itself correlated with the *Chla+b/Carx+c* (including
266 *VAZ/Chla+b*) ratio. The PRI showed a progressive decline (Fig. 7) that corresponded rather to a
267 decreasing *Chla+b/Carx+c* (Fig. 6). The third set of correlations in these PCA graphs was formed by
268 variable vectors of *A*, predawn DEPS and *Fv/Fm*. These connections placed *Fv/Fm* and predawn DEPS
269 into the role of photosynthesis predictor.

270 *Chla+b/Carx+c* plays an important role in determining both PRI₀ and midday PRI values. However, sharp
271 differences in predawn DEPS (Fig. 6) with a significant correlation with differences in ΔPRI suggested
272 that xanthophyll cycle pigment de-epoxidation was very important in the development of ΔPRI. Among
273 those factors affecting ΔPRI development, PAR was found to be a very important factor that affects
274 the magnitude of the response (Fig. 4). Although PRI₀ showed a weaker association with morning DEPS
275 (Fig. 4), the correlation between PRI₀ and predawn DEPS was nevertheless significant (research data),

276 thus confirming the importance of xanthophyll cycle pigments in the observed trends. Shifts in the
277 PRI_0 -DEPS relationship might be influenced by $Chl a+b/Carx+c$ modulating PRI value.

278 **3.3 | PRI dynamics that are consequential to photosynthesis**

279 Differences in the regulation of photosynthesis with temperature are most apparent from comparisons
280 between photosynthesis data that are measured midday (Fig. 5). Based on the observed differences,
281 relationships were developed, as shown in Fig.4. The PRI response was to a certain extent sensitive to
282 dynamic day-to-day changes in photosynthesis induced by temperature (Fig. 7), thus indicating the
283 utility of PRI for estimating dynamics of photosynthesis in fluctuating temperatures. However,
284 sensitivity to temperature-induced changes in photosynthesis did not occur within irradiance regimes
285 IRR1 and IRR2 with progressive declines in $Chl a+b/Carx+c$ (Fig. 6). The decreasing PRI in beech during
286 cold periods (second measuring days) in the IRR regimes (Fig. 7) corresponded to declining
287 photosynthesis under high-light and low-temperature conditions (Fig. 5). The further decrease in PRI
288 on the following day that was in contrast to the rising A might be related first to the increased predawn
289 DEPS and diminished PRI_0 under low-temperature conditions, consequently also resulting in a lower
290 PRI at midday (Figs. 6 and 7). The observed trend of progressively decreasing PRI with $Chl a+b/Carx+c$
291 was also observed for the spruce data set. Based on these observations we assume that the decreasing
292 PRI with $Chl a+b/Carx+c$ and cold stress was a limiting factor in enhancing the PRI response to LUE.

293 In contrast, ΔPRI showed an increase and a lower magnitude in spruce that were consistent with the
294 rise in photosynthesis upon the reduced midday temperature on measurement day 2 for each IRR
295 regime (Fig. 7). This sensitivity was the result of the increasing PRI values in spruce (Fig. 7), whereas a
296 less pronounced increase in PRI was observed in beech that was consistent with the reduced
297 photosynthesis, as shown in Fig. 9. This opposite reaction in ΔPRI in beech and spruce observed in the
298 final two measurement days for each IRR period suggested an overall increased sensitivity of ΔPRI to
299 photosynthesis (Figs. 5 and 7).

300 The inconclusive results of first-day measurements for each IRR regime might indicate possible minor
301 limitations of the applicability of Δ PRI. The low Δ PRI consistent with the high $Chl a+b/Carx+c$ on the
302 initial day of IRR1 (Fig. 6) disrupted the observed Δ PRI–LUE dependency in the spruce data. The high
303 Δ PRI amplitude in beech during the first measurement days for IRR2 and IRR3 resulted from a sudden
304 PAR increase. Closer connections between photosynthesis and Δ PRI were observed towards the end
305 of the measurements as a consequence of the diminishing $Chl a+b/Carx+c$. In addition to the observed
306 general trends, we should highlight the lowered Δ PRI in response to the higher LUE and A under later,
307 low-irradiance conditions of IRR4 that greatly strengthened the overall sensitivity of Δ PRI to LUE (Figs.
308 5 and 7). This observation thus favours Δ PRI for estimating photosynthesis responses.

309 **3.4 | Role of xanthophyll cycle pigments in the sensitivity of Δ PRI to LUE**

310 Predawn DEPS was increased under conditions of higher irradiance stress and coincided with the
311 decreasing $Chl a+b/Carx+c$ ratio and imposition of stress due to low night temperature (Figs. 4 and 6).
312 The dynamics of this response occurring on a day-to-day basis showed the rapid response of
313 xanthophyll cycle pigments to stress conditions. Nevertheless, DEPS value established during night
314 period is considered an important input requirement for accurately determining PRI_0 . Consequently
315 precisely estimated Δ PRI enables to differentiate between unstressed and stress conditions.

316 Predawn DEPS in spruce needles on the second day of the measurements within each IRR, which
317 marked the beginning of the period of dynamic temperature change, was lowered compared with the
318 values in beech and to the predawn DEPS in spruce on the first control day of the high-irradiance
319 regimes (Fig. 6). This phenomenon might be attributed to higher LAI of spruce trees, thereby providing
320 them with a greater capacity to manage excessive light in a given environment. The differences in
321 predawn DEPS were equally matched in PRI_0 values (Fig. 7). A small difference between PRI and PRI_0
322 thus indicated increased photosynthesis rates in cold temperatures under conditions of high light (Fig.
323 5). By contrast, cold night temperatures produced a high predawn DEPS, which in combination with a
324 high midday drop in PRI under high temperatures resulted in a large Δ PRI, which is consistent with a

325 drop in photosynthesis in spruce species. The reverse dynamics in pigments and PRI were observed
326 between these two days in beech (Fig. 7), concurrent with the photosynthesis dynamics (Fig. 5).

327 **3.5 | Regression analyses of PRI and Δ PRI relationships to LUE**

328 Among the observed relationships, and considering the stratifications between irradiance regimes
329 (IRR1–IRR4), the strongest relationships between PRI and LUE were observed in the dynamic light
330 environments IRR1, IRR2, and IRR4 with a changing light intensity from low to high (Table 1). The R^2
331 values for the relationship between LUE and PRI under these conditions were often as large as 0.8
332 (Table 1). The overall relationship between LUE and PRI was impacted by the decreasing
333 $Chla+b/Carx+c$, with a greater effect observed in the beech data set. By introducing Δ PRI, the overall
334 R^2 for the assessment of LUE was raised from $R^2 = 0.26$ to 0.69 in beech and from $R^2 = 0.61$ to 0.77 in
335 spruce (Fig. 8). Δ PRI failed to improve the LUE assessment in the highest irradiance period, with
336 irradiances between 900 and 1500 $\mu\text{mol m}^{-2} \text{s}^{-1}$ (IRR3, Table 1). High carotenoid levels served as a basis
337 for the effective assessment of LUE from Δ PRI in the following regime of low irradiance (IRR4) with
338 imposed low stress from irradiances in the 300–900 $\mu\text{mol m}^{-2} \text{s}^{-1}$ range. The accuracy of the LUE
339 assessment using Δ PRI in this period rose by 0.1 to $R^2 = 0.91$ and $R^2 = 0.77$ in the beech and spruce data
340 sets, respectively.

341 **4 | DISCUSSION**

342 The advantage of using Δ PRI over applying simply measured PRI for the purpose of extracting LUE has
343 been examined in this study. The presented work confirmed that the de-epoxidation cycle of leaf
344 pigments involved in NPQ has a general effect of decreasing the reflectance magnitude at wavelengths
345 around 531 nm (Gamon et al., 1990) with increasing light. The dynamics of PRI in our experimental
346 regimes of heating and cooling furthermore indicated that PRI shows an ability to track photosynthesis
347 changes in environments of fluctuating temperature. According to the measured data, the PRI-LUE
348 connection may be consequential to the connection between LUE and Φ PSII, as has been previously
349 suggested (Nichol et al., 2006; Rahimzadeh-Bajgiran et al., 2012). Although the relationship of PRI to

350 photosynthesis beyond the Φ PSII-PRI connection may be constrained by factors related to excessive
351 energy-consuming processes that are not involved in either xanthophyll cycle or carbon assimilation,
352 such as photorespiration (altered Mehler reaction and nitrate reduction) or cyclic electron transport
353 of photosystem I (PSI) (Fr chet te et al., 2015; Magney et al., 2017; Porcar-Castell et al., 2008), our
354 measurements confirm the negative interference from the slowly changing Chl_{a+b}/Car_{x+c} ratio on
355 photosynthesis estimation using PRI. The dependency of PRI on Chl_{a+b}/Car_{x+c} deteriorates the
356 relationship between PRI and LUE over the season, as previously shown by many authors (Fr chet te
357 et al., 2016; Hmimina et al., 2014; Sims and Gamon, 2002). The R^2 for the PRI–LUE relationship from
358 various plant functional types is often reported to be below 0.60, as reviewed by Garbulsky et al.
359 (2011). We were able to reach this level of connection between PRI and LUE in the spruce data set; a
360 lower R^2 of 0.26 in this relationship was estimated in beech data set, which we consider to be a
361 consequence of the lower canopy LAI of the selected beech trees resulting in higher PRI amplitudes,
362 as similar changes in Chl_{a+b}/Car_{x+c} have been estimated between species (Fig. 6).

363 There are many examples in the literature showing a negative interference from Chl_{a+b}/Car_{x+c} in LUE
364 estimation, and several studies have suggested tactics to minimize the interfering effect of
365 Chl_{a+b}/Car_{x+c} . The correction procedure may also be dependent on the application type. A detailed
366 analysis of measurements at changing observation angles and changing sun illumination angles at
367 grown canopy sites demonstrated the necessity to address dynamic reflectance changes in the canopy
368 structure and differences in the Chl_{a+b}/Car_{x+c} ratio between sunlit and shaded canopy portions
369 (Hilker et al., 2008). This research addressed the necessity to create a deconvoluting algorithm to
370 estimate LUE at each unique ecosystem station by taking into account only those PRI measurements
371 taken at certain measurement geometries from unattended spectral systems (Hilker et al., 2010). In
372 the improved approach to estimate LUE that resulted from this work, the Chl_{a+b}/Car_{x+c} ratio has
373 become regarded as an important variable indicative of canopy stress that must be accounted for –
374 and corrected – when interpreting PRI data. A group of researchers is proposing to deconvolute
375 xanthophyll-related signals by applying transformation via continuum removal of the reflectance

376 signature within the 500- to 600-nm range (Kováč et al., 2013, 2012; Woodgate et al., 2019) to
377 minimize the impact of $Chl a+b/Carx+c$ on the measurement outputs. Hernández-Clemente et al. (2011)
378 used the 512-nm band as a reference when estimating DEPS and basic physiology measures from
379 airborne data over boreal forests. The strong normalization effect of red-edge bands around 680 nm
380 for evaluating the variability of the “light-exposed” PRI has been reported in airborne data applications
381 (Zarco-Tejada et al., 2013) and when processing satellite images (Drolet et al., 2008). Ongoing research
382 continues to show that deconvoluting the early morning (predawn) state of pigments can be used to
383 reduce the impact of pigment changes on measurement outputs in applications designed to measure
384 plant stress and hence LUE (Hmimina et al., 2015; Liu et al., 2013; Ripullone et al., 2011).

385 A single PRI (PRI and PRI₀) value taken during the day is sensitive to bulk changes in $Chl a+b/Carx+c$
386 throughout the season (Garrity et al., 2011). Continuous lowering of $Chl a+b/Carx+c$ has been observed
387 in our data within each irradiance period IRR1–IRR4 (Fig. 6), thereby producing variability in PRI (Fig.
388 7). This drop in PRI has been partly helpful in determining the reduction in photosynthesis during
389 regimes IRR1–IRR3, as the decreasing LUE is associated with increasing irradiance stress, as also
390 reported by Peñuelas et al. (1995). We recognized a large interference from $Chl a+b/Carx+c$ when data
391 from low-irradiance IRR4 were included in the overall data analysis. This interference in LUE estimation
392 was removed with Δ PRI. Within the individual regimes, the relationship between PRI and LUE was
393 dependent on the observed change in xanthophyll cycle pigments following changes in irradiance
394 during the daytime period (Fig. 8, Table 1). The highest LUE-PRI connection has been achieved with
395 induced daily low to high PRI changes under conditions simulating irradiance increases from low to
396 high intensity. These conditions are similar to those used by Gamon and Surfus (1999) in their
397 pioneering study examining Δ PRI changes with DEPS. The observed trends suggest that $Chl a+b/Carx+c$
398 may be unambiguous in data across longer periods if the constitutive pigment impact on PRI is
399 efficiently discarded. Estimations of pigments at different time scales may be indirectly indicative of
400 plant stress because leaf optical properties are directly impacted by the pigment composition
401 (Peñuelas and Fillela, 1998; Wong and Gamon, 2015).

402 Deconvolution of PRI into slow-changing and fast-changing components according to Gamon and Berry
403 (2012), assuming that the “dark” component of PRI (PRI_0) is also changing between days with night
404 retention of de-epoxidized xanthophyll cycle forms (Kováč et al., 2018), narrows the LUE estimation from
405 PRI. It should be noted that our PRI measurements were based on spectral sampling at nadir
406 observations and under constant light fields so that the directional effects associated with changes in
407 illumination angles (Hernandez-Clemente et al., 2016) were small. This approach helped to narrow the
408 external factors that impact PRI, but even after removing structural effects from LAI, the PRI–LUE
409 correlation was still not strong. The ΔPRI improved the sensitivity of the measured signal to LUE across
410 multiple conditions. The variations in LUE-PRI and LUE- ΔPRI relationships were evaluated upon
411 observing temporal dynamics in species, yielding contrasting sensitivity to temperature changes (Fig.
412 5). The correction procedure unravelled the effects of $Chla+b/Carx+c$ and cold temperature on LUE
413 estimation, two main factors among three common factors impacting PRI as shown by Wong and
414 Gamon (2015). Although the spectral shift due to cold temperature was first reported as an albedo
415 shift related to changes in the physical properties of leaves in very cold temperatures (Wong and
416 Gamon, 2015), we detected low temperature interference on the LUE estimation from PRI at 12° C.
417 The shift was apparent by the decreased PRI_0 at 12° C and decreased PRI measured on the days
418 following the application of cold stress (Fig. 7). In the context of our measurements, the shift appears
419 to be only partly related to the high DEPS.

420 A predictive pattern of decreasing PRI towards midday was typically observed in our testing data set
421 when the temperature increase followed the PAR increase (Fig. 2). By comparing dynamic PRI changes
422 in response to experimental temperature lowering (Fig. 9), we endeavoured to identify the change in
423 PRI in response to the increased photosynthetic efficiency in spruce and to low temperature stress in
424 beech trees. It is well known that the observed PRI dynamic changes within a matter of minutes to
425 hours result from the synergy between xanthophyll cycle pigment conversions and management of
426 the energetic carriers ATP and NADPH under changing conditions (Nichol et al., 2000), thereby
427 producing signal variation with photosynthesis efficiency. We detected an increase in PRI in spruce in

428 response to enhanced photosynthesis reactions (Fig. 9). As a consequence of enhancing photo
429 protection in beech, a less-pronounced increase in PRI was measured (Fig. 9), resulting in a decreased
430 PRI compared with the photosynthetically more efficient spruce. Similar PRI responses to the
431 photosynthesis changes induced in the diurnal frame have been reported by Gamon et al. (1992), who
432 examined differences in PRI between control, nutrient-stressed and water-stressed sunflower leaves.
433 In our experiment, feedback between PRI and photosynthetic reactions was detected, which greatly
434 improved the accuracy of Δ PRI in tracking dynamic photosynthetic changes with induced temperature
435 variations.

436 However, the studies of Δ PRI do not involve variations in this signal caused by the canopy structure,
437 which may render leaf traits difficult to discern (Knyazikhin et al., 2012). Magney et al. (2016)
438 postulated that Δ PRI affords limited improvements in decoupling the structural (LAI) effect from the
439 raw PRI signal, and thereby, PRI_0 is primarily sensitive to variability in pigment content and should not
440 be used to correct for changes in LAI. For efficient disentangling of the desirable effect in Δ PRI to match
441 its value with photosynthesis, an accurate assessment of PRI_0 that is consistent with the dynamics in
442 DEPS was required (Figs. 6 and 7). Particularly, PRI_0 estimation on the second measurement days for
443 each irradiance regime is considered a crucial factor for development of the observed LUE- Δ PRI.
444 However, examining aspects of PRI_0 and Δ PRI estimation on these days revealed importance of LAI in
445 the observed relationships, resulting from determinations of sapling capacity to manage the available
446 light (Ellsworth and Reich, 1993). Assessment of the PRI_0 signal is based on the dependency of PRI on
447 the de-epoxidation state of xanthophyll cycle pigments (Gamon et al., 1990), and night-time levels of
448 DEPS are often influenced by temperature and induced stress (Demmig-Adams and Adams, 1996;
449 Gilmore and Björkman, 1995). The causality of the relationship between Δ PRI and LUE appears to be a
450 consequence of the differences in canopies LAI between species and levels of imposed stress. The
451 results highlight the importance of estimating PRI_0 that matches DEPS and a highly complex nature of
452 the mechanisms involved in remote assessments of photosynthesis change, underscoring the need for
453 very precise data.

454 By concept, Δ PRI appears to be a suitable tool for observing the dynamics of changes within small areas
455 of vegetated surfaces throughout day periods to monitor short-term variations in leaf pigments.
456 Further assuming the field application of presented Δ PRI concept, difficulties may arise when isolating
457 PRI_0 in early morning field reflectance measurements. The errors in estimation may originate from the
458 cosine response of the diffusers used and from the relative variation in the measured signal of the total
459 down-welling radiance flux. Variations in measured incoming radiation flux are caused by deviations
460 in the measurement of direct and diffuse components of the down-welling flux passing through the
461 diffusers (Pacheco-Labrador et al., 2019). The fraction of diffuse irradiance is usually low in remote-
462 sensing applications if the cloudy data are discarded, but the contribution of diffuse irradiance can be
463 large in the case of automated proximal sensing comparing data on a large temporal scale and
464 including measurements acquired at low and high sun elevations (Gamon et al., 2015; Pacheco-
465 Labrador and Martín, 2015). Estimating PRI_0 and PRI from reflectance data may be challenging due to
466 the unknown directional distribution of the diffuse irradiance. Most applications have been set up for
467 PRI_0 from measurements that have occurred in a period around 9 a.m. when the solar zenith is around
468 or greater than 40° (Liu et al., 2013; Magney et al., 2016) and the sun is potentially yielding a higher
469 intensity. This phenomenon may be considered a consequence of the observed cosine response in the
470 measured data. Improvements in instrumentation for the measurements may also be required to
471 reproduce data with higher standards.

472 The results highlight a great diversity of parameters to which PRI measurements may refer in beech
473 and spruce forests. They also show that PRI is highly comparable to indicators based on relative units
474 such as Φ_{PSII} , LUE, or the $Chla+b/Carx+c$ ratio, and that assessment of LUE can be improved with the
475 use of Δ PRI, which uses the balance between PRI and PRI_0 . The involvement of protection mechanisms
476 that are not involved in any of the NPQ mechanisms may be a reason for the weakened correlation
477 between Δ PRI and NPQ, but the weaker PRI–NPQ connection is often a result of the $Chla+b/Carx+c$
478 adjustments to light conditions (Stylinski et al., 2002). It can be presumed that the strong association
479 between variables is a result of applying artificial light, which minimizes fluctuations of PRI, Φ_{PSII} , NPQ,

480 and LUE in the data set, as reported by Sukhov and Sukhova (2018). For the practical problem of field
481 remote sensing, the results show that the application of PRI can be effective for investigating
482 photosynthesis in dynamic irradiance and temperature regimes if the pigments are sufficiently
483 disentangled in the signal. The presented work may serve as premise for data processing if interfering
484 factors in spectral measurements in the field are efficiently reduced. However, measurements of
485 control plants that have not been affected by stressors are often necessary to establish the
486 dependency of optic parameters on observed factors (Damm et al., 2018; Sukhova and Sukhov, 2018).

487 **CONCLUSION**

488 The results showed that photosynthesis estimation using PRI over periods longer than days may be
489 limited by changing dynamics of the foliar Chl_{a+b}/Car_{x+c} ratio with stress from irradiance. The extent
490 of the Chl_{a+b}/Car_{x+c} limitation in our measurements was dependent on the leaf area index of the
491 measured trees; we recorded greater interference from Chl_{a+b}/Car_{x+c} in beech seedlings with a lower
492 LAI. An improved assessment of dynamic changes in photosynthetic activity induced with changes in
493 irradiance and temperature was achieved using ΔPRI . The measurements also showed the importance
494 of foliage and environmental factors for the observed dynamics in PRI. The estimation of ΔPRI was
495 based on measuring PRI_0 under low irradiance. Temperature was considered a factor that induces
496 changes in xanthophyll cycle pigment DEPS observed in PRI. The improved approach as proposed by
497 introducing ΔPRI may deconvolute part of the interference in the PRI signal. The limitations of the ΔPRI
498 may be related to changes in this signal with sudden increases in irradiance when evaluating canopies
499 with a lower LAI. Low foliar amounts of xanthophyll cycle pigments may render a low amplitude of
500 ΔPRI , which was a minor limiting factor when evaluating our spruce dataset. Conversely, on days
501 starting with low temperature, ΔPRI was effective in disentangling the negative effect caused by low
502 temperature on the photosynthesis estimation. Other stresses and less predictive patterns of
503 environmental changes may exist in the field; the mechanism should be further tested under various
504 conditions.

505 **ACKNOWLEDGEMENTS**

506 This work was supported by the Ministry of Education, Youth, and Sports of the Czech Republic within
507 the National Infrastructure for Carbon Observations-CzeCOS (No. LM2015061) and SustES –
508 Adaptation strategies for sustainable ecosystem services and food security under adverse
509 environmental conditions (CZ.02.1.01/0.0/0.0/16_019/0000797). JP also acknowledges funding from
510 European Research Council Synergy grant ERC-SyG-2013-610028 IMBALANCE-P.

511 **REFERENCES**

512 Coops, N.C., Hermosilla, T., Hilker, T., Andrew Black, T., 2017. Linking stand architecture with canopy
513 reflectance to estimate vertical patterns of light-use efficiency. *Remote Sens. Environ.* 194,
514 322–330. doi:10.1016/j.rse.2017.03.025

515 Damm, A., Paul-Limoges, E., Haghghi, E., Simmer, C., Morsdorf, F., Schneider, F.D., van der Tol, C.,
516 Migliavacca, M., Rascher, U., 2018. Remote sensing of plant-water relations: An overview and
517 future perspectives. *J. Plant Physiol.* 227, 3–19. doi:10.1016/j.jplph.2018.04.012

518 Demmig-Adams, B., Adams, W., 1996. The role of xanthophyll cycle carotenoids in the protection of
519 photosynthesis. *Trends Plant Sci.* 1, 21–26. doi:10.1016/S1360-1385(96)80019-7

520 Drolet, G.G., Middleton, E.M., Huemmrich, K.F., Hall, F.G., Amiro, B.D., Barr, A.G., Black, T.A.,
521 Mccaughey, J.H., Margolis, H.A., 2008. Remote Sensing of Environment Regional mapping of
522 gross light-use efficiency using MODIS spectral indices. *Remote Sens. Environ.* 112, 3064–3078.
523 doi:10.1016/j.rse.2008.03.002

524 Ellsworth, D.S., Reich, P.B., 1993. Canopy structure and vertical patterns of photosynthesis and
525 related leaf traits in a deciduous forest. *Oecologia* 96, 169–178. doi:10.1007/BF00317729

526 Filella, I., Porcar-Castell, A., Munné-Bosch, S., Bäck, J., Garbulsky, M.F., Peñuelas, J., 2009. PRI
527 assessment of long-term changes in carotenoids/chlorophyll ratio and short-term changes in

528 de-epoxidation state of the xanthophyll cycle. *Int. J. Remote Sens.* 30, 4443–4455.
529 doi:10.1080/01431160802575661

530 Fréchette, E., Chang, C.Y.Y., Ensminger, I., 2016. Photoperiod and temperature constraints on the
531 relationship between the photochemical reflectance index and the light use efficiency of
532 photosynthesis in *Pinus strobus*. *Tree Physiol.* 36, 311–324. doi:10.1093/treephys/tpv143

533 Fréchette, E., Wong, C.Y.S., Junker, L.V., Chang, C.Y.Y., Ensminger, I., 2015. Zeaxanthin-independent
534 energy quenching and alternative electron sinks cause a decoupling of the relationship between
535 the photochemical reflectance index (PRI) and photosynthesis in an evergreen conifer during
536 spring. *J. Exp. Bot.* 66, 7309–7323. doi:10.1093/jxb/erv427

537 Gamon, J.A., Berry, J.A., 2012. Facultative and constitutive pigment effects on the Photochemical
538 Reflectance Index (PRI) in sun and shade conifer needles [WWW Document]. *Isr. J. Plant Sci.*
539 doi:10.1560/IJPS.60.1-2.85

540 Gamon, J.A., Bond, B., 2013. Effects of irradiance and photosynthetic downregulation on the
541 photochemical reflectance index in Douglas-fir and ponderosa pine. *Remote Sens. Environ.* 135,
542 141–149. doi:10.1016/j.rse.2013.03.032

543 Gamon, J.A., Field, C.B., Bilger, W., Björkman, O., Fredeen, A.L., Peñuelas, J., 1990. Remote sensing of
544 the xanthophyll cycle and chlorophyll fluorescence in sunflower leaves and canopies. *Oecologia*
545 85, 1–7. doi:10.1007/BF00317336

546 Gamon, J.A., Kovalchuck, O., Wong, C.Y.S., Harris, A., Garrity, S.R., 2015. Monitoring seasonal and
547 diurnal changes in photosynthetic pigments with automated PRI and NDVI sensors.
548 *Biogeosciences* 12, 4149–4159. doi:10.5194/bg-12-4149-2015

549 Gamon, J.A., Peñuelas, J., Field, C.B., 1992. A narrow-waveband spectral index that tracks diurnal
550 changes in photosynthetic efficiency. *Remote Sens. Environ.* doi:10.1016/0034-4257(92)90059-

551 S

552 Gamon, J.A., Serrano, L., Surfus, J.S., 1997. The photochemical reflectance index: An optical indicator
553 of photosynthetic radiation use efficiency across species, functional types, and nutrient levels.
554 *Oecologia* 112, 492–501. doi:10.1007/s004420050337

555 Gamon, J.A., Surfus, J.S., 1999. Assessing leaf pigment content and activity with a reflectometer. *New*
556 *Phytol.* 143, 105–117. doi:10.1046/j.1469-8137.1999.00424.x

557 Garbulsky, M.F., Peñuelas, J., Gamon, J., Inoue, Y., Filella, I., 2011. The photochemical reflectance
558 index (PRI) and the remote sensing of leaf, canopy and ecosystem radiation use efficiencies. A
559 review and meta-analysis. *Remote Sens. Environ.* doi:10.1016/j.rse.2010.08.023

560 Garbulsky, M.F., Peñuelas, J., Papale, D., Filella, I., 2008. Remote estimation of carbon dioxide uptake
561 by a Mediterranean forest. *Glob. Chang. Biol.* 14, 2860–2867. doi:10.1111/j.1365-
562 2486.2008.01684.x

563 Garrity, S.R., Eitel, J.U.H., Vierling, L.A., 2011. Disentangling the relationships between plant pigments
564 and the photochemical reflectance index reveals a new approach for remote estimation of
565 carotenoid content. *Remote Sens. Environ.* 115, 628–635. doi:10.1016/j.rse.2010.10.007

566 Genty, B., Briantais, J.M., Baker, N.R., 1989. The relationship between the quantum yield of
567 photosynthetic electron transport and quenching of chlorophyll fluorescence. *Biochim. Biophys.*
568 *Acta* 990, 87–92.

569 Gilmore, A.M., Björkman, O., 1995. Temperature-sensitive coupling and uncoupling of ATPase-
570 mediated, nonradiative energy dissipation: Similarities between chloroplasts and leaves. *Planta*
571 197, 646–654. doi:10.1007/BF00191573

572 Gilmore, A.M., Björkman, O., 1994. Adenine nucleotides and the xanthophyll cycle in leaves - II.
573 Comparison of the effects of CO₂- and temperature-limited photosynthesis on photosystem II

574 fluorescence quenching, the adenylate energy charge and violaxanthin de-epoxidation in
575 cotton. *Planta* 192, 537–544. doi:10.1007/BF00203592

576 Gitelson, A.A., Gamon, J.A., Solovchenko, A., 2017. Remote Sensing of Environment Multiple drivers
577 of seasonal change in PRI : Implications for photosynthesis 2 . Stand level. *Remote Sens.*
578 *Environ.* 190, 198–206. doi:10.1016/j.rse.2016.12.015

579 Hernandez-Clemente, R., Kolari, P., Porcar-Castell, A., Korhonen, L., Mottus, M., 2016. Tracking the
580 Seasonal Dynamics of Boreal Forest Photosynthesis Using EO-1 Hyperion Reflectance:
581 Sensitivity to Structural and Illumination Effects. *IEEE Trans. Geosci. Remote Sens.* 54, 5105–
582 5116. doi:10.1109/TGRS.2016.2554466

583 Hernández-Clemente, R., Navarro-Cerrillo, R.M., Suárez, L., Morales, F., Zarco-Tejada, P.J., 2011.
584 Assessing structural effects on PRI for stress detection in conifer forests. *Remote Sens. Environ.*
585 115, 2360–2375. doi:10.1016/j.rse.2011.04.036

586 Hilker, T., Coops, N.C., Hall, F.G., Black, T.A., Wulder, M.A., Nesic, Z., Krishnan, P., 2008. Separating
587 physiologically and directionally induced changes in PRI using BRDF models. *Remote Sens.*
588 *Environ.* 112, 2777–2788. doi:10.1016/j.rse.2008.01.011

589 Hilker, T., Hall, F.G., Coops, N.C., Lyapustin, A., Wang, Y., Nesic, Z., Grant, N., Black, T.A., Wulder,
590 M.A., Kljun, N., Hopkinson, C., Chasmer, L., 2010. Remote sensing of photosynthetic light-use
591 efficiency across two forested biomes: Spatial scaling. *Remote Sens. Environ.* 114, 2863–2874.
592 doi:10.1016/j.rse.2010.07.004

593 Hmimina, G., Dufrêne, E., Soudani, K., 2014. Relationship between photochemical reflectance index
594 and leaf ecophysiological and biochemical parameters under two different water statuses:
595 Towards a rapid and efficient correction method using real-time measurements. *Plant, Cell*
596 *Environ.* 37, 473–487. doi:10.1111/pce.12171

- 597 Hmimina, G., Merlier, E., Dufrêne, E., Soudani, K., 2015. Deconvolution of pigment and physiologically
598 related photochemical reflectance index variability at the canopy scale over an entire growing
599 season. *Plant, Cell Environ.* 38, 1578–1590. doi:10.1111/pce.12509
- 600 Knyazikhin, Y., Schull, M.A., Stenberg, P., Möttus, M., Rautiainen, M., Yang, Y., 2012. Hyperspectral
601 remote sensing of foliar nitrogen content. *Proc. Natl. Acad. Sci.* 110, 185–192.
602 doi:10.1073/pnas.1210196109
- 603 Kováč, D., Malenovský, Z., Urban, O., Špunda, V., Kalina, J., Ač, A., Kaplan, V., Hanuš, J., 2013.
604 Response of green reflectance continuum removal index to the xanthophyll de-epoxidation
605 cycle in Norway spruce needles. *J. Exp. Bot.* 64, 1817–1827.
- 606 Kováč, D., Navrátil, M., Malenovský, Z., Štroch, M., Špunda, V., Urban, O., 2012. Reflectance
607 continuum removal spectral index tracking the xanthophyll cycle photoprotective reactions in
608 Norway spruce needles. *Funct. Plant Biol.* 39, 987–998. doi:10.1071/FP12107
- 609 Kováč, D., Veselovská, P., Klem, K., Večeřová, K., Ač, A., Peñuelas, J., Urban, O., 2018. Potential of
610 Photochemical Reflectance Index for Indicating Photochemistry and Light Use Efficiency in
611 Leaves of European Beech and Norway Spruce Trees. *Remote Sens.* 10, 1202.
612 doi:10.3390/rs10081202
- 613 Kurasová, I., Kalina, J., Urban, O., Štroch, M., Špunda, V., 2003. Acclimation of two distinct plant
614 species, spring barley and Norway spruce, to combined effect of various irradiance and CO₂
615 concentration during cultivation in controlled environment. *Photosynthetica* 41, 513–523.
616 doi:10.1023/B:PHOT.0000027515.05641.fd
- 617 Lichtenthaler, H.K., 1987. Chlorophylls and carotenoids: Pigments of photosynthetic biomembranes.
618 *Methods Enzymol.* 148, 350–382. doi:10.1016/0076-6879(87)48036-1
- 619 Liu, L., Zhang, Y., Jiao, Q., Peng, D., 2013. Assessing photosynthetic light-use efficiency using a solar-

620 induced chlorophyll fluorescence and photochemical reflectance index. *Int. J. Remote Sens.* 34,
621 4264–4280. doi:10.1080/01431161.2013.775533

622 Magney, T.S., Frankenberg, C., Fisher, J.B., Sun, Y., North, G.B., Davis, T.S., Kornfeld, A., Siebke, K.,
623 2017. Methods Connecting active to passive fluorescence with photosynthesis : a method for
624 evaluating remote sensing measurements of Chl fluorescence. *New Phytol.* 215, 1594–1608.
625 doi:10.1111/nph.14662

626 Magney, T.S., Vierling, L.A., Eitel, J.U.H., Huggins, D.R., Garrity, S.R., 2016. Response of high frequency
627 Photochemical Reflectance Index (PRI) measurements to environmental conditions in wheat.
628 *Remote Sens. Environ.* 173, 84–97. doi:10.1016/j.rse.2015.11.013

629 Middleton, E.M., Cheng, Y., Hilker, T., Black, T.A., Krishnan, P., Coops, N.C., Huemmrich, K.F., 2009.
630 Linking Foliage Spectral Responses to Canopy Level Ecosystem Photosynthetic Linking foliage
631 spectral responses to canopy-level ecosystem photosynthetic light-use efficiency at a Douglas-
632 fir forest in Canada. *Can. J. Remote Sens.* 35, 166–188. doi:10.5589/m09-008

633 Nichol, C.J., Huemmrich, K.F., Black, T.A., Jarvis, P.G., Walthall, C.L., Grace, J., Hall, F.G., 2000. Remote
634 sensing of photosynthetic-light-use efficiency of boreal forest. *Agric. For. Meteorol.* 101, 131–
635 142. doi:10.1016/S0168-1923(99)00167-7

636 Nichol, C.J., Rascher, U., Matsubara, S., Osmond, B., 2006. Assessing photosynthetic efficiency in an
637 experimental mangrove canopy using remote sensing and chlorophyll fluorescence. *Trees -*
638 *Struct. Funct.* 20, 9–15. doi:10.1007/s00468-005-0005-7

639 Niinemets, Ü., Valladares, F., 2004. Photosynthetic acclimation to simultaneous and interacting
640 environmental stresses along natural light gradients: Optimality and constraints. *Plant Biol.*
641 doi:10.1055/s-2004-817881

642 Ollinger, S. V, 2011. Sources of variability in canopy reflectance and the convergent properties of

643 plants. *New Phytol.* 189, 375–394.

644 Pacheco-Labrador, J., Hueni, A., Mihai, L., Sakowska, K., Julitta, T., Kuusk, J., Sporea, D., Alonso, L.,
645 Burkart, A., Cendrero-Mateo, Aasen, H., Goulas, Y., Mac Arthur, A., 2019. Sun-Induced
646 Chlorophyll Fluorescence I: Instrumental Considerations for Proximal Spectroradiometers.
647 *Remote Sens.* 11, 960. doi:10.3390/rs11080960

648 Pacheco-Labrador, J., Martín, M.P., 2015. Characterization of a field spectroradiometer for
649 unattended vegetation monitoring. Key sensor models and impacts on reflectance. *Sensors* 15,
650 4154–4175. doi:10.3390/s150204154

651 Peñuelas, J., Filella, I., Gamon, J. a, 1995. Assessment of photosynthetic radiation-use efficiency with
652 spectral reflectance. *New Phytol.* 131, 291–296. doi:10.1111/j.1469-8137.1995.tb03064.x

653 Peñuelas, J., Fillela, I., 1998. Visible and near-infrared reflectance techniques for diagnosing plant
654 physiological status. *Trends Plant Sci.* 3, 151–156.

655 Peñuelas, J., Garbulsky, M.F., Filella, I., 2011. Photochemical reflectance index (PRI) and remote
656 sensing of plant CO₂ uptake. *New Phytol.* doi:10.1111/j.1469-8137.2011.03791.x

657 Porcar-Castell, A., Juurola, E., Ensminger, I., Berninger, F., Hari, P., Nikinmaa, E., 2008. Seasonal
658 acclimation of photosystem II in *Pinus sylvestris*. II. Using the rate constants of sustained
659 thermal energy dissipation and photochemistry to study the effect of the light environment.
660 *Tree Physiol.* 28, 1483–1491. doi:10.1093/treephys/28.10.1483

661 R Core Team, 2018. R: A Language and Environment for Statistical Computing. (R Foundation for
662 Statistical Computing: Vienna, Austria). Available at <https://www.R-project.org/>

663 Rahimzadeh-Bajgiran, P., Munehiro, M., Omasa, K., 2012. Relationships between the photochemical
664 reflectance index (PRI) and chlorophyll fluorescence parameters and plant pigment indices at
665 different leaf growth stages, in: *Photosynthesis Research*. pp. 261–271. doi:10.1007/s11120-

666 012-9747-4

667 Rascher, U., Agati, G., Alonso, L., Cecchi, G., Champagne, S., Colombo, R., Damm, A., Daumard, F., De
668 Miguel, E., Fernandez, G., Franch, B., Franke, J., Gerbig, C., Gioli, B., Gómez, J.A., Goulas, Y.,
669 Guanter, L., Gutiérrez-De-La-Cámara, É., Hamdi, K., Hostert, P., Jiménez, M., Kosvancova, M.,
670 Lognoli, D., Meroni, M., Miglietta, F., Moersch, A., Moreno, J., Moya, I., Neininger, B., Okujeni,
671 A., Ounis, A., Palombi, L., Raimondi, V., Schickling, A., Sobrino, J.A., Stellmes, M., Toci, G.,
672 Toscano, P., Udelhoven, T., Van Der Linden, S., Zaldei, A., 2009. CEFLES2: The remote sensing
673 component to quantify photosynthetic efficiency from the leaf to the region by measuring sun-
674 induced fluorescence in the oxygen absorption bands. *Biogeosciences* 6, 1181–1198.
675 doi:10.5194/bg-6-1181-2009

676 Ripullone, F., Rivelli, A.R., Baraldi, R., Guarini, R., Guerrieri, R., Magnani, F., Peñuelas, J., Raddi, S.,
677 Borghetti, M., 2011. Effectiveness of the photochemical reflectance index to track
678 photosynthetic activity over a range of forest tree species and plant water statuses. *Funct. Plant*
679 *Biol.* 38, 177–186. doi:10.1071/FP10078

680 Sims, D.A., Gamon, J.A., 2002. Relationships between leaf pigment content and spectral reflectance
681 across a wide range of species, leaf structures and developmental stages. *Remote Sens. Environ.*
682 81, 337–354. doi:10.1016/S0034-4257(02)00010-X

683 Sims, D.A., Luo, H., Hastings, S., Oechel, W.C., Rahman, A.F., Gamon, J.A., 2006. Parallel adjustments
684 in vegetation greenness and ecosystem CO₂ exchange in response to drought in a Southern
685 California chaparral ecosystem. *Remote Sens. Environ.* 103, 289–303.
686 doi:10.1016/j.rse.2005.01.020

687 Soudani, K., Hmimina, G., Dufrêne, E., Berveiller, D., Delpierre, N., Ourcival, J.M., Rambal, S., Joffre,
688 R., 2014. Relationships between photochemical reflectance index and light-use efficiency in
689 deciduous and evergreen broadleaf forests. *Remote Sens. Environ.* 144, 73–84.

690 doi:10.1016/j.rse.2014.01.017

691 Stylinski, C.D., Gamon, J.A., Oechel, W.C., 2002. Seasonal patterns of reflectance indices, carotenoid
692 pigments and photosynthesis of evergreen chaparral species. *Oecologia* 131, 366–374.
693 doi:10.1007/s00442-002-0905-9

694 Sukhova, E., Sukhov, V., 2018. Connection of the photochemical reflectance index (PRI) with the
695 photosystem II quantum yield and nonphotochemical quenching can be dependent on
696 variations of photosynthetic parameters among investigated plants: A meta-analysis. *Remote*
697 *Sens.* 10, 771. doi:10.3390/rs10050771

698 Williams, M., Rastetter, E.B., Fernandez, D.N., Goulden, M.L., Wofsy, S.C., Shaver, G.R., Melillo, J.M.,
699 Munger, J.W., Fan, S.-M., Nadelhoffer, K.J., 1996. Modelling the soil-plant-atmosphere
700 continuum in a *Quercus*–*Acer* stand at Harvard Forest: the regulation of stomatal conductance
701 by light, nitrogen and soil/plant hydraulic properties. *Plant. Cell Environ.* 19, 911–927.
702 doi:10.1111/j.1365-3040.1996.tb00456.x

703 Wong, C.Y.S., Gamon, J.A., 2015. Three causes of variation in the photochemical reflectance index
704 (PRI) in evergreen conifers. *New Phytol.* 206, 187–195. doi:10.1111/nph.13159

705 Woodgate, W., Suarez, L., Gorsel, E. Van, Cernusak, L.A., Dempsey, R., Devilla, R., Held, A., Hill, M.J.,
706 Norton, A.J., 2019. tri-PRI : A three band reflectance index tracking dynamic photoprotective
707 mechanisms in a mature eucalypt forest. *Agric. For. Meteorol.* 272–273, 187–201.
708 doi:10.1016/j.agrformet.2019.03.020

709 Wu, C., Huang, W., Yang, Q., Xie, Q., 2015. Improved estimation of light use efficiency by removal of
710 canopy structural effect from the photochemical reflectance index (PRI). *Agric. Ecosyst. Environ.*
711 199, 333–338. doi:10.1016/j.agee.2014.10.017

712 Zarco-Tejada, P.J., González-Dugo, V., Williams, L.E., Suárez, L., Berni, J.A.J., Goldhamer, D., Fereres,

713 E., 2013. A PRI-based water stress index combining structural and chlorophyll effects:
714 Assessment using diurnal narrow-band airborne imagery and the CWSI thermal index. Remote
715 Sens. Environ. 138, 38–50. doi:10.1016/j.rse.2013.07.024

716

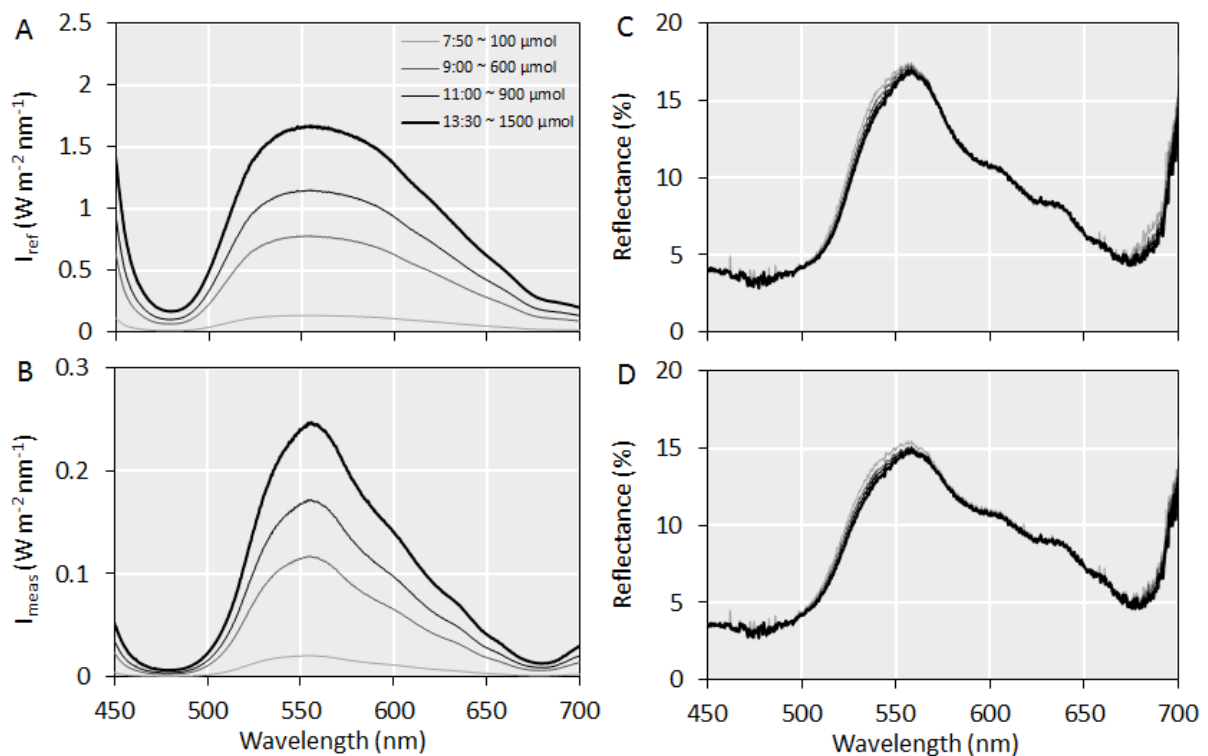
717

718

719

720

721



722

723

724 **Fig. 1** (A) Spectral intensity emitted by white LED panels (I_{ref}) in growth chambers under four
725 photosynthetically active radiation (PAR) intensities: 100, 600, 900, and 1500 $\mu mol m^{-2} s^{-1}$; (B)

726 spectral intensity reflected from spruce saplings under corresponding PAR intensities (I_{meas});
727 reflectance spectra of European beech (C) and Norway spruce (D) saplings under corresponding
728 irradiances in one day during the IRR2 regime.

729

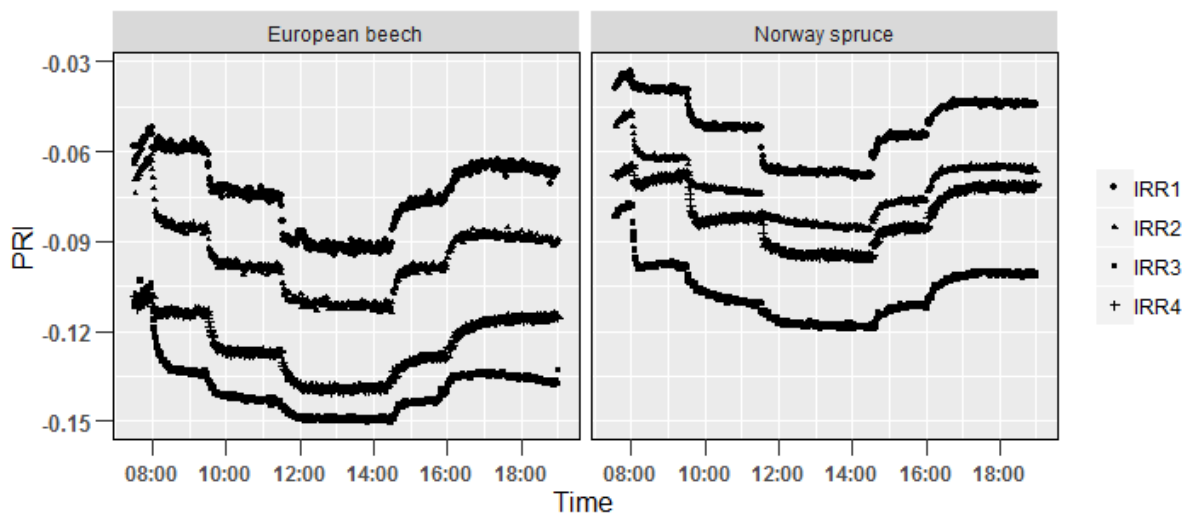
730

731

732

733

734



736 **Fig. 2** PRI dynamics on the control (normal) day of each irradiance regime (IRR1, IRR2, IRR3, IRR4) as
737 measured for beech and spruce canopies.

738

739

740

741

742

743

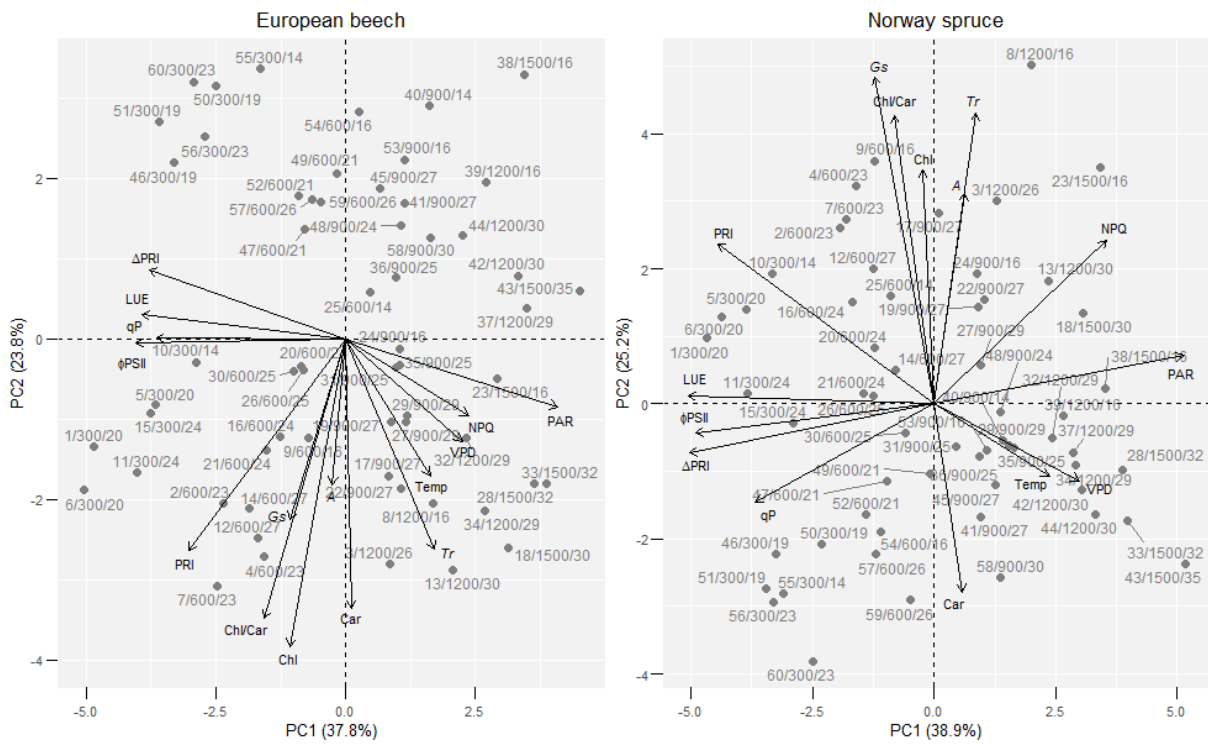
744

745

746

747

748



749

750 **Fig. 3** Biplot of variables and individuals measured showing interactions among spectral information

751 (PRI and ΔPRI), environmental conditions (PAR, Temp, VPD) inside growth chambers, and gas exchange

752 (A, Gs, Tr, LUE), active fluorescence (Φ_{PSII}, NPQ, qP), and foliar pigment (Chl, Car, Chl /Car)

753 characteristics of the examined vegetation. Individual data points are labelled to indicate the number

754 of measurements taken/irradiance/temperature. A group of 5 measurements represent data collected
 755 on one day of measurement. A total of 60 values from 12 measurement days in leaves of spruce and
 756 beech trees are shown.

757

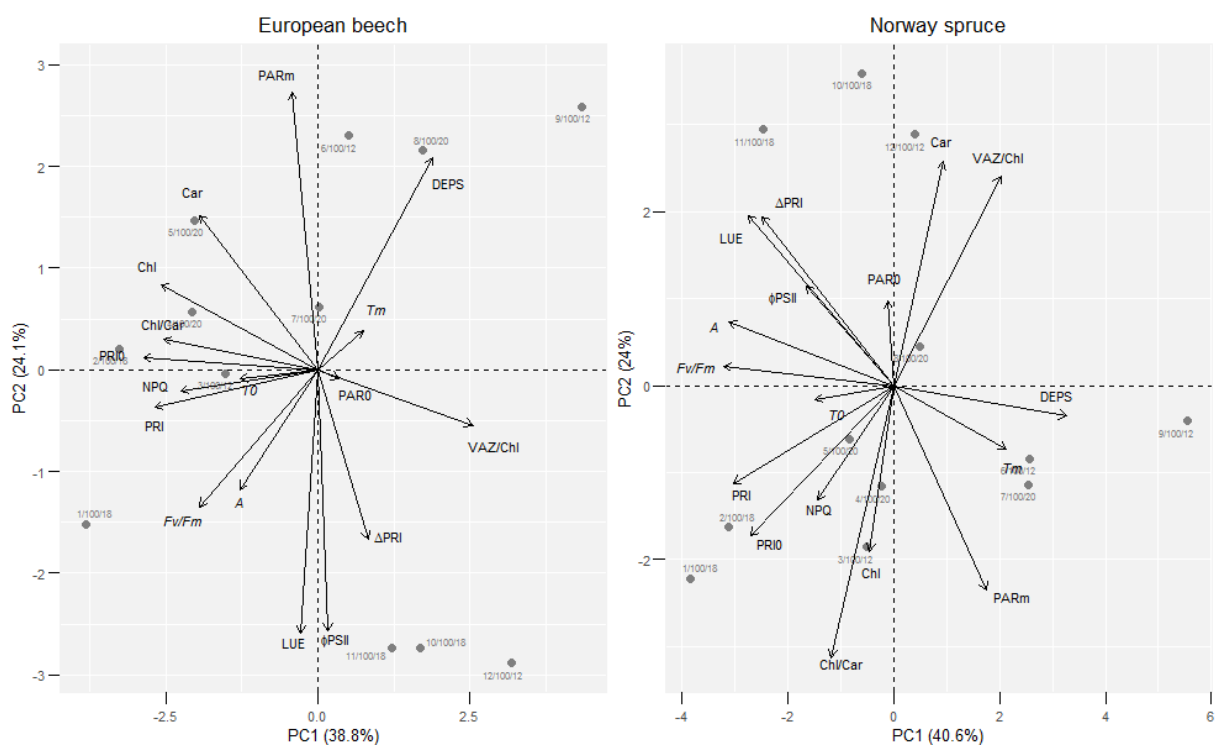
758

759

760

761

762



763

764 **Fig. 4** Biplots of variables and individuals for measurement days (n = 12) of beech and spruce trees
 765 showing interactions among foliar pigments (Chl/Car, VAZ/Chl, predawn DEPS), spectral information
 766 (PRI₀, midday PRI, ΔPRI), environmental conditions (PAR₀, midday PAR_m, overnight T₀, and midday

767 temperature, T_m), and key physiology measures estimated both predawn (F_v/F_m) and during midday
768 (A , LUE, Φ_{PSII} , NPQ). Individual data points are labelled with the measurement day number/irradiance
769 at dawn/night temperature.

770

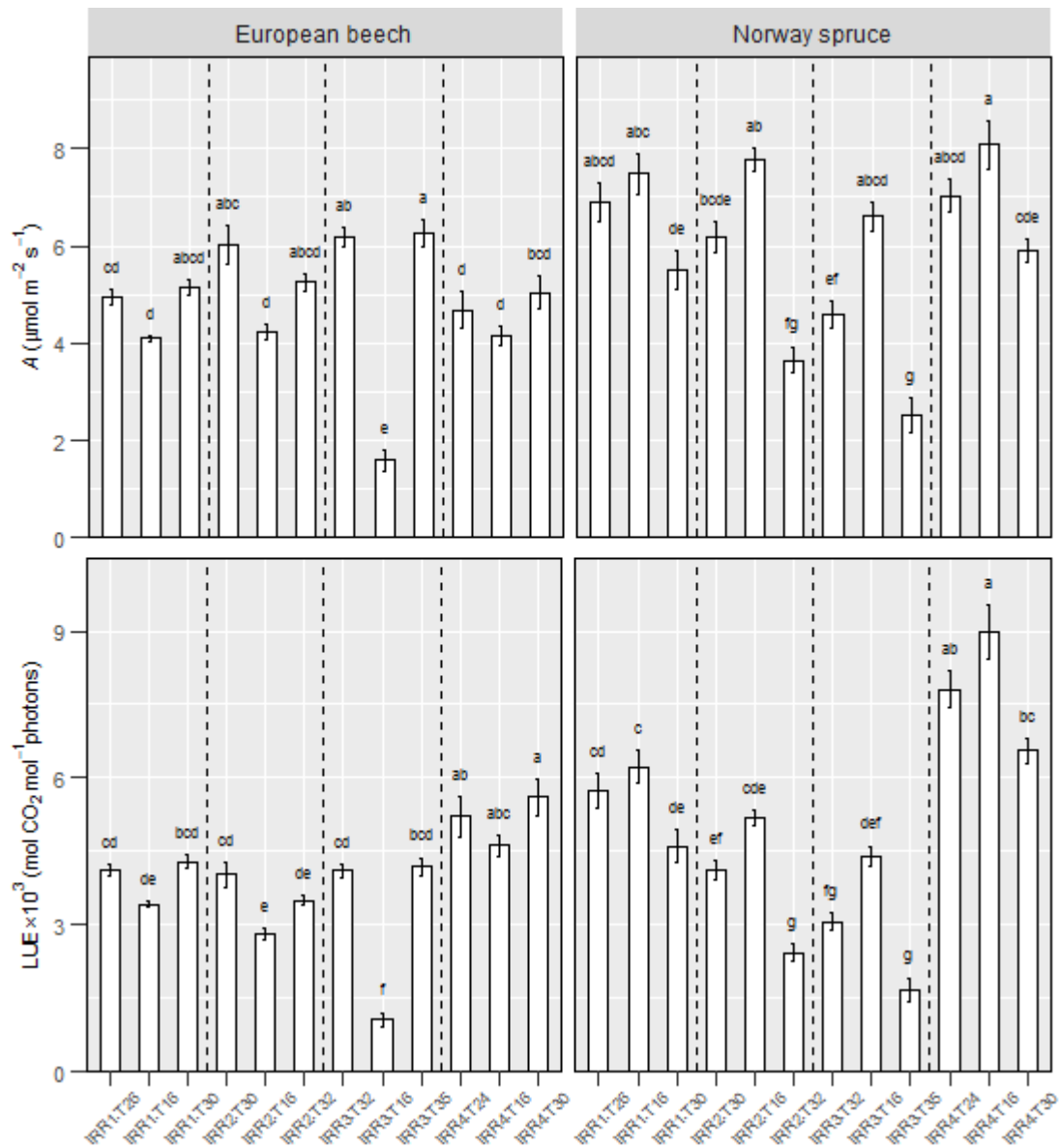
771

772

773

774

775

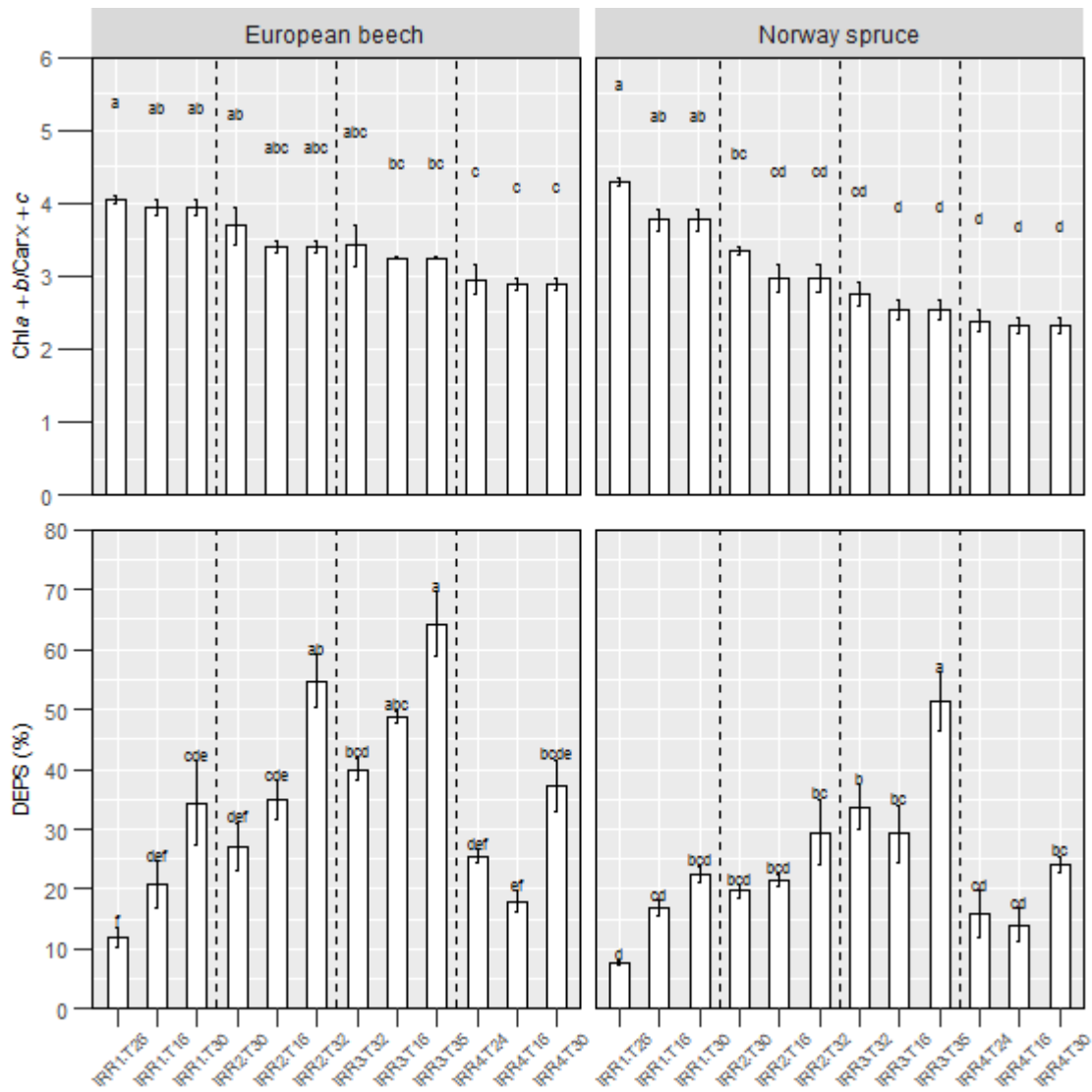


776

777 **Fig. 5** Photosynthetic capacity (A) and light use efficiency (LUE) in leaves of beech and spruce at
 778 midday of measurement days under four irradiance regimes (IRR1–IRR4). IRR period label and midday
 779 temperature indicate irradiance-and-temperature conditions during the measurements. Means and
 780 standard deviations (error bars) of the measurements are presented ($n = 6$). Letters indicate
 781 homogeneous groups ($p < 0.05$; Tukey's post hoc test). Different letters above the bars indicate
 782 statistically significant differences between means.

783

784



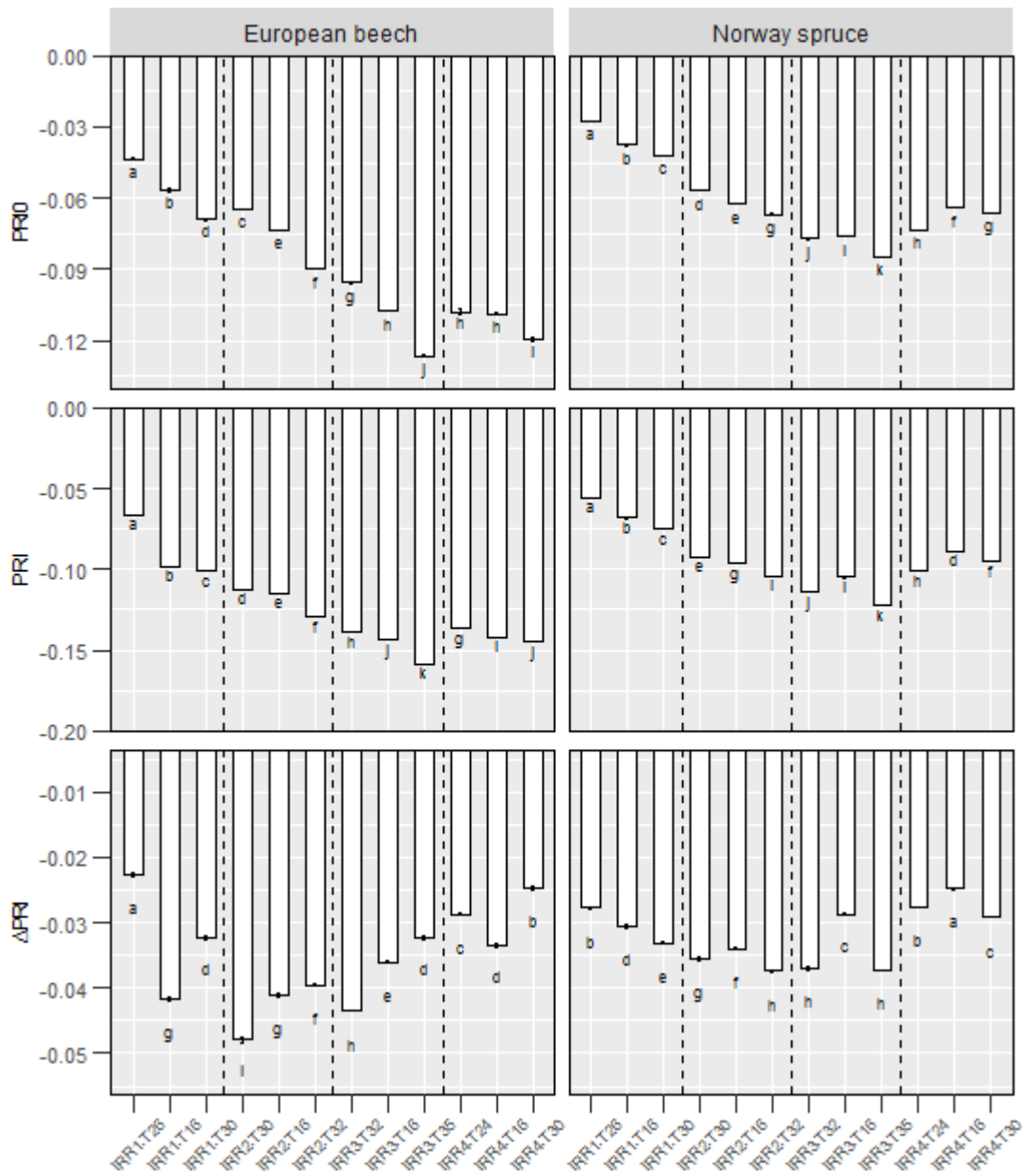
785

786 **Fig. 6** Ratio of chlorophylls to carotenoids and de-epoxidation state of xanthophyll cycle pigments
 787 (DEPS) estimated for leaves of darkness-acclimated beech and spruce trees on days of physiological
 788 measurements. Means and standard deviations (error bars) of the measurements are presented ($n =$
 789 3). Letters indicate homogeneous groups ($p < 0.05$; Tukey's post hoc test). Different letters above the
 790 bars indicate statistically significant differences between the means.

791

792

793



794

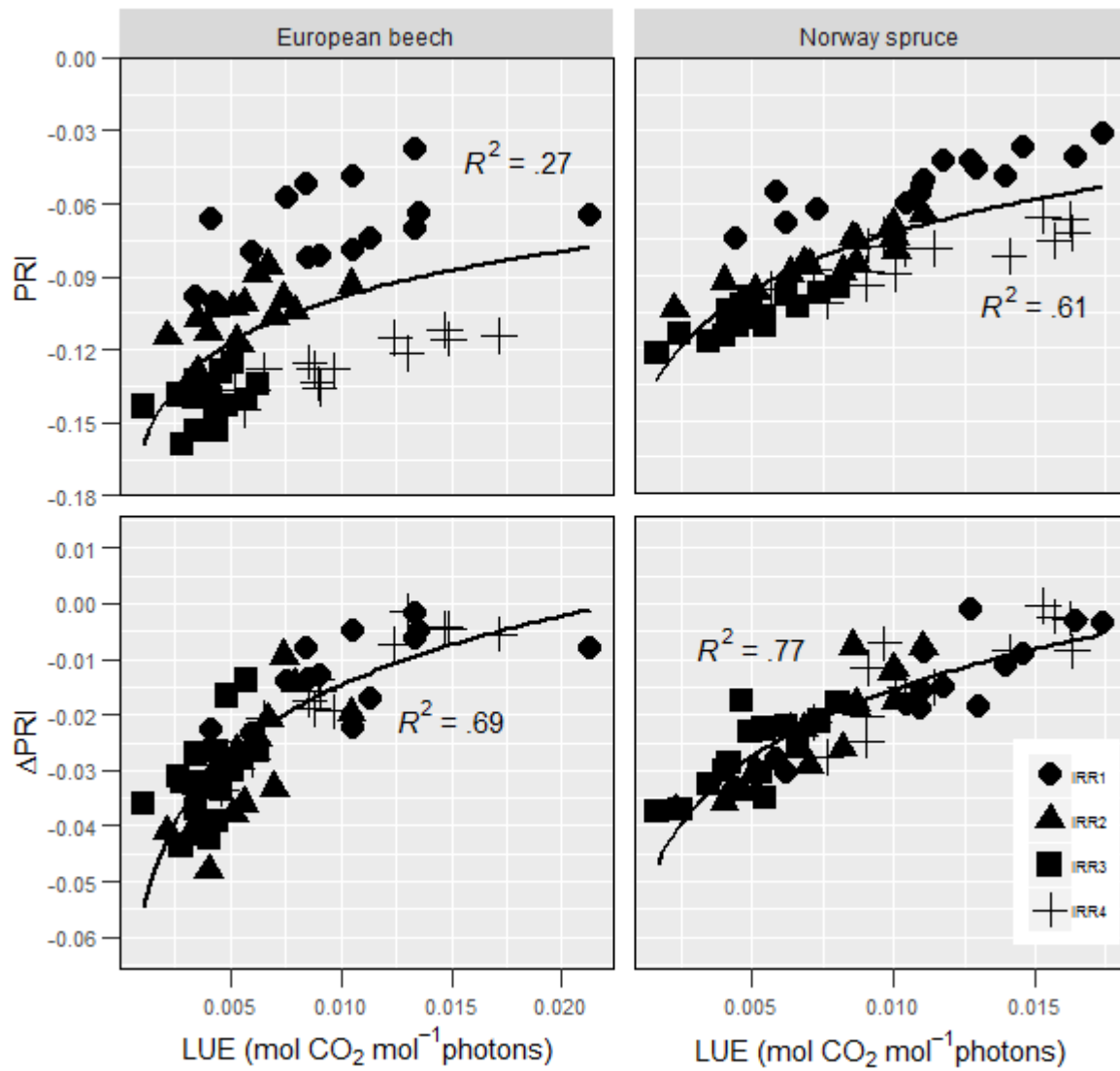
795 **Fig. 7** Development of early morning PRI₀, midday PRI, and differential ΔPRI in changing midday
 796 temperature conditions under four irradiance regimes (IRR1–IRR4), separated by broken lines. Letters
 797 indicate homogeneous groups ($p < 0.05$; $n = 6$; Tukey's post hoc test).

798

799

800

801



802

803 **Fig. 8** Relationships between LUE and PRI (Δ PRI) in all data measured during all four irradiance regimes
 804 (IRR1–IRR4). Coefficients of determination for overall relationships between variables are displayed in
 805 the figure ($n = 60$).

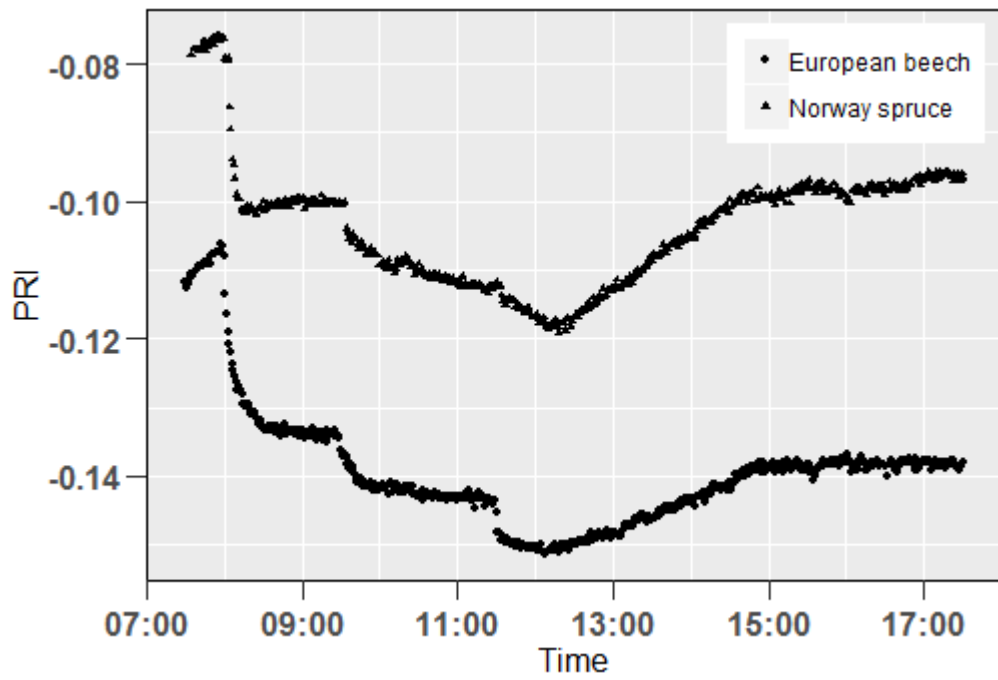
806

807

808

809

810



811

812 **Fig. 9** PRI dynamics on a measurement day with midday cooling to 16 °C during the highest-irradiance
 813 regime, IRR3. Physiology measurements and optical data to report PRI during the midday period were
 814 taken at 14:00. Cooling of trees started at 12:00.

815

816

817

818

819

820

821

822

823 **Table 1** Coefficients of determination (R^2) for PRI-LUE and Δ PRI-LUE relationships in beech and spruce
 824 saplings as observed in Fig. 8. Relationships estimated for data pairs estimated in four individual IRR
 825 regimes ($n = 15$) and among all measured data ($n = 60$). The significance of the results was tested at
 826 levels $*p < 0.05$, $**p < 0.01$, and $***p < 0.001$; ns indicates a non-significant result

827

IRR regime	European beech		Norway spruce	
	PRI-LUE	Δ PRI-LUE	PRI-LUE	Δ PRI-LUE
IRR1	0.30*	0.68***	0.79***	0.81***
IRR2	0.36*	0.54***	0.77***	0.74***
IRR3	0.07 ^{ns}	0.20 ^{ns}	0.71***	0.53***
IRR4	0.82***	0.91***	0.62***	0.77***
Total	0.27***	0.69***	0.61***	0.77***

828

829

830 **Table 2** Fitting logarithmic equations for PRI-LUE and Δ PRI-LUE relationships in beech and spruce
 831 saplings as observed in Fig. 8. Coefficients of determination for these relationships are shown in table
 832 1. Equations were estimated for data pairs estimated in four individual IRR regimes ($n = 15$) and among
 833 all measured data ($n = 60$)

IRR regime	European beech		Norway spruce	
	PRI-LUE	Δ PRI-LUE	PRI-LUE	Δ PRI-LUE
IRR1	$y=0.0191\ln(x)+0.0202$	$y=0.0181\ln(x)+0.0701$	$y=0.0267\ln(x)+0.0702$	$y=0.0221\ln(x)+0.0852$
IRR2	$y=0.0177\ln(x)+0.0128$	$y=0.0197\ln(x)+0.0738$	$y=0.0229\ln(x)+0.0296$	$y=0.0198\ln(x)+0.0764$
IRR3	$y=0.0057\ln(x)+0.1091$	$y=0.0087\ln(x)+0.0176$	$y=0.0164\ln(x)+0.0188$	$y=0.0119\ln(x)+0.0362$
IRR4	$y=0.0230\ln(x)+0.0191$	$y=0.0232\ln(x)+0.0931$	$y=0.0255\ln(x)+0.0344$	$y=0.0249\ln(x)+0.0991$
Total	$y=0.0027\ln(x)+0.0259$	$y=0.0179\ln(x)+0.0678$	$y=0.0339\ln(x)+0.0836$	$y=0.0175\ln(x)+0.0655$

834

835